Volume 58
Number 86
7 November 2022
Pages 12005–12128

ChemComm

Chemical Communications

rsc.li/chemcomm

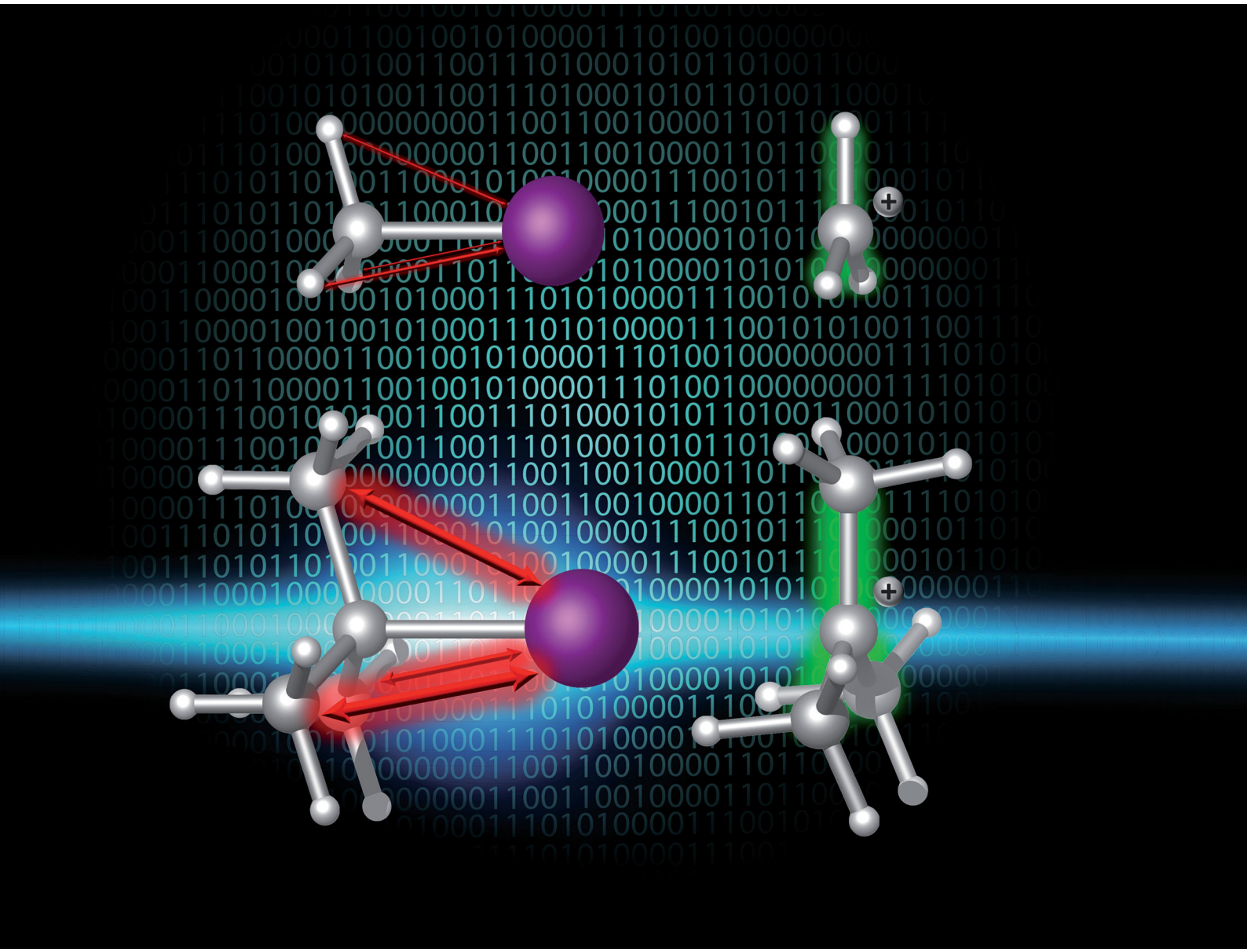

ISSN 1359-7345

ROYAL SOCIETY OF CHEMISTRY

COMMUNICATION

Thomas Hansen, F. Matthias Bickelhaupt, Trevor A. Hamlin *et al.*

Stability of alkyl carbocations

ChemComm

COMMUNICATION

View Article Online
View Journal | View Issue

Cite this: *Chem. Commun.*, 2022, **58**, 12050

Received 19th July 2022,
Accepted 6th October 2022

DOI: 10.1039/d2cc04034d

rsc.li/chemcomm

Stability of alkyl carbocations†

Thomas Hansen, *[ab] Pascal Vermeeren, [a] F. Matthias Bickelhaupt *[ac] and Trevor A. Hamlin *[a]

The traditional and widespread rationale behind the stability trend of alkyl-substituted carbocations is incomplete. Through state-of-the-art quantum chemical analyses, we quantitatively established a generally overlooked driving force behind the stability of carbocations, namely, that the parent substrates are substantially destabilized by the introduction of substituents, often playing a dominant role in solution. This stems from the repulsion between the substituents and the C–X bond.

Carbocations are ubiquitous reactive intermediates in synthetic chemistry and are involved in many fundamental organic transformations.[1,2] These reactive intermediates generally form through a heterolytic C–X bond dissociation, yielding a carbocation C^+ and an anionic X^-. The heterolytic bond dissociation energy (BDE), for simple alkyl halides $Me_mH_{3-m}C$–X, decreases upon increasing methyl substitution along the series of H_3C–X (methyl, 0°), MeH_2C–X (primary, 1°), Me_2HC–X (secondary, 2°), Me_3C–X (tertiary, 3°).[3] In other words, it is easier to form more substituted carbocations, making them more likely to participate as an intermediate in a chemical reaction.

Currently, the reduced heterolytic bond dissociation energy of the C–X bond is often ascribed to the stabilization of the carbocation, which increases along methyl, primary, secondary, and tertiary substituted carbocations.[4] This stability trend stems from the stabilizing interactions (hyperconjugation and inductive effects)[1a,5] between the electron-depleted carbon center and the methyl groups. The true definition of structural stability is less straightforward than stated above since, strictly speaking, one cannot directly compare the structural stabilities of non-isomeric species.[6,7] Furthermore, this trend also has been attributed to the relief of steric repulsion, going from the substrate to the carbocation, between the substituents of the C–X bond for more substituted systems (also known as B-strain; back-strain).[8]

Typically, the thermodynamic stability of organic molecules is quantified using hypothetical reactions (*e.g.*, isodesmic or homodesmotic), which are specifically designed to isolate a desired effect.[9] Recently, in contrast to common textbook knowledge, we found using isodesmic reactions that methyl substitution destabilizes simple organic radicals.[10] In our present study, we partition the energy of the system using the isodesmic reaction shown in eqn (1), which allows us to investigate the effect of the number of methyl groups on the thermodynamic stability of the system. We use the non-substituted H_3C–X as our reference compound. This approach has proven useful for quantifying the stability of organic molecules, however, it does not directly permit one to uncover the true origin of the stability trend.

$$H_3C\text{–}X + Me_mH_{3-m}C^+ \rightarrow H_3C^+ + Me_mH_{3-m}C\text{–}X \qquad (1)$$

Herein, we reveal the exact source of the stability trend of carbocations by using partial reactions in a thermodynamic cycle quantitatively decomposing the effect of methyl groups on the carbocation species and the parent substrate, as shown in Scheme 1 (purple bonds). We have chosen to study the archetypal $Me_mH_{3-m}C$–X model systems with m = 0, 1, 2, 3 and X = F, Cl, Br, I, H, CH_3. The activation strain model (ASM)[11] was employed to provide quantitative insight into the driving processes for the carbocation stability.

Here, we focus on the $Me_mH_{3-m}C$–I systems as a representative example. However, all model systems we have studied, that is, $Me_mH_{3-m}C$–X (m = 0–3; X = F, Cl, Br, H, CH_3), possess

[a] *Department of Theoretical Chemistry, Amsterdam Institute of Molecular and Life Sciences (AIMMS), Amsterdam Center for Mul-tiscale Modeling (ACMM), Vrije Universiteit Amsterdam, De Boelelaan 1083, 1081 HV Amsterdam, The Netherlands. E-mail: t.hansen@vu.nl, t.a.hamlin@vu.nl*

[b] *Departament de Química Inorgànica i Orgànica (Secció de Química Orgànica) & Institut de Química Teòrica i Computacional (IQTCUB), Universitat de Barcelona, 08028 Barcelona, Spain. E-mail: f.m.bickelhaupt@vu.nl*

[c] *Institute for Molecules and Materials (IMM), Radboud University, Heyendaalseweg 135, 6525 AJ Nijmegen, The Netherlands*

† Electronic supplementary information (ESI) available: Additional computational results; Cartesian coordinates, energies, and the number of imaginary frequencies of all stationary points. See DOI: https://doi.org/10.1039/d2cc04034d

Scheme 1 Computationally studied heterolytic bond dissociation of the C–X bond (R = H or Me; X = F, Cl, Br, I, H, CH_3).

similar trends and can be found in Table S1 and Fig. S1 (ESI†). Table 1 presents our computed $Me_mH_{3-m}C$–I bond lengths (r (C–I)) and heterolytic bond dissociation enthalpies (ΔH_{BDE}^{hetero}). The dissociation of the leaving-group atom, X^-, from the tetrahedral substrate leads to a $Me_mH_{3-m}C^+$ carbocation. The latter adopts a trigonal planar geometry to optimize the $C^{+\bullet\bullet\bullet}$-substituent bonding overlap between the singly-occupied 2p atomic orbitals of C^+ and the E-symmetric SOMO of the substituents $R_3^{\bullet\bullet\bullet}$ (where a dot $^\bullet$ represents an unpaired electron; see Fig. S2 for structures, ESI†). The trigonal planar geometry also minimizes steric (Pauli) repulsion between the substituents. Note that, as reported earlier, the ethyl cation adopts a ''non-classical'' bridged carbocation structure in which the positive charge is delocalized over both carbons (see Fig. S2, ESI†).[12]

As expected, the C–I bond, indeed, significantly weakens as the degree of methyl substitution increases, going from ΔH_{BDE}^{hetero} = 210.7 to 170.1 to 152.5 to 137.2 kcal mol^{-1}, along m = 0, 1, 2, and 3 (see Table 1). At the same time, the C–I bond also becomes longer along this series from 2.132 to 2.150 to 2.170 to 2.194 Å. Our computed bond dissociation energies at ZORA-M06-2X/QZ4P are in good agreement with experiments (see Table S2, ESI†).[3] Moreover, the same general conclusions are obtained at ZORA-BLYP-D3(BJ)/QZ4P and ZORA-BP86-D3(BJ)/QZ4P, see Fig. S3, S4 and Tables S3, S4 (ESI†).

To analyze how the heterolytic $Me_mH_{3-m}C$–X bond dissociation enthalpy depends on both the bonding of the substituents in the carbocation $Me_mH_{3-m}C^+$ and in its parent substrate $Me_mH_{3-m}C$–X, we have decomposed the heterolytic bond dissociation enthalpy of the system into three terms: ΔH_{Parent}(X, m), $\Delta H_{BDE}^{hetero}(C^{\bullet\bullet\bullet}\text{–X})$, and $\Delta H_{Cation}(m)$ (eqn (2)), associated with the three partial reactions of the thermochemical cycle shown in Table 1. The ΔH_{Parent}(X, m) is the overall bond enthalpy as the three separate substituents, *i.e.*, $Me_mH_{3-m}^{\bullet\bullet\bullet}$ combine with $C^{\bullet\bullet\bullet}$–X to form the parent substrate $Me_mH_{3-m}C$–X. The $\Delta H_{BDE}^{hetero}(C^{\bullet\bullet\bullet}\text{–X})$ is the heterolytic C–X bond dissociation enthalpy of the completely unsubstituted $C^{\bullet\bullet\bullet}$–X species into $C^{+\bullet\bullet\bullet}$ and X^-. The $\Delta H_{Cation}(m)$ is the overall bond enthalpy as the three separate substituents $Me_mH_{3-m}^{\bullet\bullet\bullet}$ combine with $C^{+\bullet\bullet\bullet}$ to form the carbocation $Me_mH_{3-m}C^+$. Thus, we have the following relationship of eqn (2):

$$\Delta H_{BDE}^{hetero} = \Delta H_{BDE}^{hetero}(C^{\bullet\bullet\bullet}\text{–X}) + \Delta H_{Cation}(m) - \Delta H_{Parent}(X, m) \quad (2)$$

Consequently, the trend in isodesmic dissociation energy ($\Delta\Delta H_{BDE}^{hetero}$) upon increasing methyl substitution is determined not only by $\Delta\Delta H_{Cation}(m)$ but by the difference between $\Delta\Delta H_{Cation}(m)$ and $\Delta\Delta H_{Parent}$(X, m) (eqn (3)–(5)). In other words, a less stable parent molecule is more prone to dissociate the leaving-group and hence form a carbocation.

$$\Delta\Delta H_{Cation}(m) = \Delta H_{Cation}(m) - \Delta H_{Cation}(m = 0) \quad (3)$$

$$\Delta\Delta H_{Parent}(X, m) = \Delta H_{Parent}(X, m) - \Delta H_{Parent}(X, m = 0) \quad (4)$$

$$\Delta\Delta H_{BDE}^{hetero} = \Delta\Delta H_{Cation}(m) - \Delta\Delta H_{Parent}(X, m) \quad (5)$$

Several trends emerge from our decomposition of ΔH_{BDE}^{hetero} using the thermochemical cycle in Table 1 (Fig. 1). As discussed previously, the $Me_mH_{3-m}C$–I bonds become weaker by increasing the number of methyl groups, which is illustrated by the increasingly more negative isodesmic dissociation energy ($\Delta\Delta H_{BDE}^{hetero}$) in Fig. 1a (black line). We find that the parent substrate $Me_mH_{3-m}C$–I is systematically destabilized by the substituents, as seen in Fig. 1a (blue line) by the positive $\Delta\Delta H_{Parent}$(X, m) going from +10.0 to +18.8 to +27.0 kcal mol^{-1} along m = 1, 2, 3. In contrast, the carbocation is stabilized by the substituents (red line), through, among others, hyperconjugation, as evidenced by the more stabilizing $\Delta\Delta H_{Cation}(m)$ going from −30.5 to −39.5 to −46.5 kcal mol^{-1} along the same series.

To assess the role of solvation, we have also studied the decomposition of ΔH_{BDE}^{hetero} in solution with COSMO. For this purpose, we selected dichloromethane (ε = 9), DMSO (ε = 47), and water (ε = 78), spanning realistic extremes of polarity used in experiments.[13] For our discussion, we focus on water solvation and note that in all solvents, the same general trends emerge, see Tables S5, S6 and Fig. S5 (ESI†).

Solvation significantly reduces the stabilizing effects of the methyl groups on the carbocation (Fig. 1c, red line) with $\Delta\Delta H_{Cation}(m)$(aq) of only −16.1, −17.2, −19.2 kcal mol^{-1} going from m = 1 to 2 to 3, respectively. This stems from the fact that the less substituted carbocation, with its more localized and

Table 1 R_3C–X (R = H or Me; X = I) bond lengths (in Å) and heterolytic bond dissociation energies (ΔH_{BDE}^{hetero}), which are decomposed using a thermochemical cycle in ΔH_{Parent}(X, m), $\Delta H_{BDE}^{hetero}(C^{\bullet\bullet\bullet}\text{–X})$, and $\Delta H_{Cation}(m)$ (kcal mol^{-1})[a]

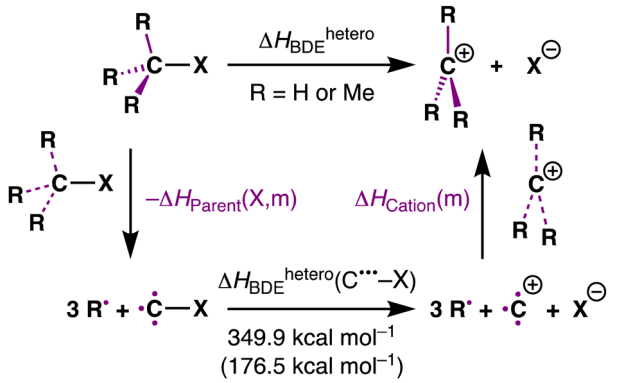

System	r (C–X)	ΔH_{BDE}^{hetero}	ΔH_{Parent}(X, m)	$\Delta H_{Cation}(m)$
H_3C–I	2.132 (2.136)	210.7 (66.7)	−321.5 (−320.8)	−453.0 (−440.2)
MeH_2C–I	2.150 (2.157)	170.1 (40.1)	−311.5 (−310.3)	−483.5 (−456.3)
Me_2HC–I	2.170 (2.181)	152.5 (29.8)	−302.7 (−301.1)	−492.4 (−457.7)
Me_3C–I	2.194 (2.209)	137.2 (19.2)	−294.5 (−292.4)	−499.5 (−459.4)

[a] Computed at ZORA-(U)M06-2X/QZ4P and values in parentheses at COSMO(H_2O)-ZORA-(U)M06-2X/QZ4P, at 298.15 K and 1 atm.

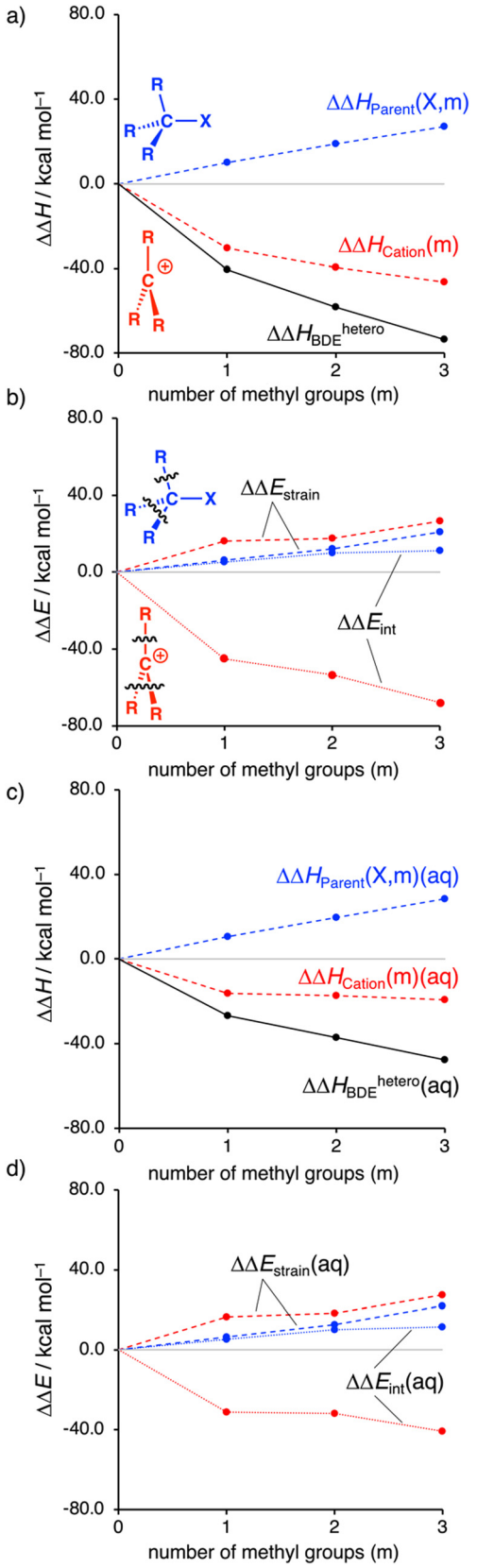

Fig. 1 Effect of methyl groups on $\Delta\Delta H_{BDE}^{hetero}$, $\Delta\Delta H_{Parent}$(X, *m*), $\Delta\Delta H_{Cation}$(m), and the corresponding activation strain analysis (in kcal mol^{-1}) for R_3C–X (R = H or Me; X = I). Computed at ZORA-(U)M06-2X/QZ4P (a and b) and COSMO(H_2O)-ZORA-(U)M06-2X/QZ4P (c and d).

less shielded positive charge, enters into a more stabilizing interaction with the solvent. In sharp contrast, the observed systematic destabilization of the parent substrate $Me_mH_{3-m}C$–I by the substituents is entirely maintained if we go from the gas phase to solution, as reflected by $\Delta\Delta H_{Parent}$(X, *m*)(aq), which still steeply increases from +10.1, +19.7, +28.4 kcal mol^{-1} along the same series.

Note that, in solution, the magnitude of stabilization of the carbocation levels off after the addition of more than one methyl group. This saturation effect finds its origin in the aforementioned interaction between the solvated cation and the substituents. Introducing the first substituent stabilizes the cation, reducing the electron depletion on the carbocation. Intuitively, the next substituent can interact less strongly with the less depleted pertinent carbon center. This effect is also observed in the gas phase, although less apparent.

Next, to further understand the effect of the methyl groups on the carbocation stability, we employ our activation strain model (see ESI† for Computational methods; Fig. 1b and d).[9] Note that the computed trends are the same for both ΔH and ΔE (Table S1, ESI†). We continue with the analysis of ΔE. As discussed, the parent substrate is systematically destabilized by adding methyl groups, which can be traced back to both the destabilizing strain ($\Delta\Delta E_{strain} > 0$) and less stabilizing interaction energy ($\Delta\Delta E_{int} > 0$; Fig. 1b). The less stabilizing interaction energy stems from the substituents that engage in steric (Pauli) repulsive interactions (see Fig. S6 and S7, ESI†). The larger methyl groups have more repulsion with the C$^{\bullet\bullet\bullet}$–X bond and have more mutual repulsion than the smaller hydrogen atoms. This type of repulsion is also known as F-strain (front-strain).[14] The destabilizing strain mainly results from the need of the methyl group(s) to deform from their planar methyl radical equilibrium geometry to a pyramidal geometry in the substrate.[15]

In contrast, the carbocation becomes more stabilized by the introduction of substituents, which stems from the stabilizing interactions between the substituents and the cationic carbon center (Fig. 1b). Our quantitative MO analyses show that this, indeed, finds its origin in, among others, the stabilizing hyperconjugation (Fig. S8 and S9, ESI†). For the carbocations, a systematically slightly more destabilizing strain compared to the parent substrate is found (Fig. 1b; red *versus* blue dashed line). This can be traced back to the intrinsically shorter carbon–substituent bonds for the carbocations, which require the methyl groups to deform more. The shorter carbon–substituent bonds of the trigonal planar carbocations are a result of the relief of steric repulsion between the substituents.

Note that the jump in both the interaction and strain energy by going from the methyl to the ethyl cation is the direct effect of the "non-classical" bridged carbocation (see Fig. S6 and S7, ESI†). As discussed above, solvation stabilizes the carbocation and thus reduces the electron-accepting capabilities of this species (attenuates hyperconjugative effects), which leads to a substantial reduction of the substituent–cation interaction going from the gas phase to solution (Fig. 1d). While the destabilizing steric repulsive effects in the systems are maintained.

In conclusion, we find that the heterolytic bond strength of C–X bonds decreases as the degree of alkyl substitution increases. We quantitatively established a commonly overlooked driving force behind this trend, namely, the parent substrate is increasingly destabilized by introducing alkyl substituents. This is the result of destabilizing steric repulsion between the alkyl substituents and the C–X bond (also known as F-strain). This trend is reinforced by the stabilization of the carbocation by the alkyl substituents through, among others, hyperconjugation. We found that the destabilization of the parent substrate often plays a dominant role if the species are in solution.

Conflicts of interest

There are no conflicts to declare.

Notes and references

1 (*a*) D. H. Aue, *Wiley Interdiscip. Rev.: Comput. Mol. Sci.*, 2011, **4**, 487; (*b*) R. R. Naredla and D. A. Klumpp, *Chem. Rev.*, 2013, **113**, 6905; (*c*) D. J. Tantillo, *Nat. Prod. Rep.*, 2011, **28**, 1035; (*d*) D. J. Tantillo, *Chem. Soc. Rev.*, 2010, **39**, 2847; (*e*) X. Creary, *Chem. Rev.*, 1991, **91**, 1625; (*f*) M. Saunders and H. A. Jimenez-Vazquez, *Chem. Rev.*, 1991, **91**, 375; (*g*) G. I. Borodkin, I. R. Elanov and V. G. Shubin, *Russ. J. Org. Chem.*, 2021, **57**, 301.

2 (*a*) J. Bah, V. R. Naidu, J. Teske and J. Franzén, *Adv. Synth. Catal.*, 2015, **357**, 148; (*b*) J. P. Richard, T. L. Amyes and M. M. Toteva, *Acc. Chem. Res.*, 2001, **34**, 981; (*c*) T. Hansen, L. Lebedel, W. A. Remmerswaal, S. van der Vorm, D. P. A. Wander, M. Somers, H. S. Overkleeft, D. V. Filippov, J. Désiré, A. Mingot, Y. Bleriot, G. A. van der Marel, S. Thibaudeau and J. D. C. Codée, *ACS Cent. Sci.*, 2019, **5**, 781; (*d*) M. A. Mercadante, C. B. Kelly, T. A. Hamlin, K. R. Delle Chiaie, M. D. Drago, K. K. Duffy, M. T. Dumas, D. C. Fager, B. L. C. Glod, K. E. Hansen, C. R. Hill, R. M. Leising, C. L. Lynes, A. E. MacInnis, M. R. McGohey, S. A. Murray, M. C. Piquette, S. L. Roy, R. M. Smith, K. R. Sullivan, B. H. Truong, K. M. Vailonis, V. Gorbatyuk, N. E. Leadbeater and L. J. Tilley, *Chem. Sci.*, 2014, **5**, 3983; (*e*) S. van der Vorm, T. Hansen, E. R. van Rijssel, R. Dekkers, J. M. Madern, H. S. Overkleeft, D. V. Filippov, G. A. van der Marel and J. D. C. Codée, *Chem. – Eur. J.*, 2019, **25**, 7149; (*f*) E. S. Stoyanov, I. V. Stoyanova, F. S. Tham and C. A. Reed, *Angew. Chem., Int. Ed.*, 2012, **51**, 9149; (*g*) J. M. Madern, T. Hansen, E. R. van Rijssel, H. A. V. Kistemaker, S. van der Vorm, H. S. Overkleeft, G. A. van der Marel, D. V. Filippov and J. D. C. Codée, *J. Org. Chem.*, 2019, **8**, 1218.

3 (*a*) Y. R. Luo and P. D. Pacey, *J. Phys. Chem.*, 1991, **95**, 9470; (*b*) H. M. Rosenstock, R. Buff, M. A. Ferreira, S. G. Lias, A. C. Parr, R. L. Stockbauer and J. L. Holmes, *J. Am. Chem. Soc.*, 1982, **104**, 2337; (*c*) E. M. Arnett and N. J. Pienta, *J. Am. Chem. Soc.*, 1980, **102**, 3329–3334.

4 (*a*) F. A. Carey and R. J. Sundberg, *Advanced Organic Chemistry Part A: Structure and Mechanisms*, Springer, 5 edn, 2007, pp. 300–310; (*b*) M. B. Smith, *March's Advanced Organic Chemistry: Reactions, Mechanisms, and Structure*, 6th edn, Wiley, New York, 2013, pp. 234–245; (*c*) F. P. Lossing and J. L. Holmes, *J. Am. Chem. Soc.*, 1984, **106**, 6917.

5 (*a*) E. S. Stoyanov and G. dos Passos Gomes, *J. Phys. Chem. A*, 2015, **119**, 8619; (*b*) I. V. Alabugin, G. dos Passos Gomes and M. A. Abdo, *Wiley Interdiscip. Rev.: Comput. Mol. Sci.*, 2019, e1389; (*c*) I. V. Alabugin, K. M. Gilmore and P. W. Peterson, *Wiley Interdiscip. Rev.: Comput. Mol. Sci.*, 2011, **1**, 109.

6 (*a*) M. L. Coote, A. Pross and L. Radom, *Org. Lett.*, 2003, **5**, 4689; (*b*) M. Swart, E. Rösler and F. M. Bickelhaupt, *Eur. J. Inorg. Chem.*, 2007, 3646; (*c*) C. Rüchardt, *Angew. Chem., Int. Ed. Engl.*, 1970, **9**, 830; (*d*) K. B. Clark and D. D. M. Wayner, *J. Am. Chem. Soc.*, 1991, **113**, 9363; (*e*) S. Gronert, *J. Org. Chem.*, 2006, **71**, 1209; (*f*) S. Gronert, *J. Org. Chem.*, 2006, **71**, 7045; (*g*) S. Gronert, *Org. Lett.*, 2007, **9**, 2211; (*h*) M. Swart and F. M. Bickelhaupt, *J. Chem. Theory Comput.*, 2006, **2**, 281; (*i*) F. M. Bickelhaupt, H. L. Hermann and G. Boche, *Angew. Chem., Int. Ed.*, 2006, **45**, 823.

7 (*a*) A. A. Zavitsas, *J. Chem. Educ.*, 2001, **78**, 417; (*b*) J. L. M. Abboud, I. Alkorta, J. Z. Davalos, P. Müller, E. Quintanilla and J. C. Rossier, *J. Org. Chem.*, 2003, **68**, 3786; (*c*) P. de, A. M. Nicholas and D. R. Arnold, *Can. J. Chem.*, 1984, **62**, 1850.

8 (*a*) T. Sorrell, *Organic Chemistry*, 2 edn, 2006, pp 186–188; (*b*) K. Takeuchi, Y. Ohga and T. Kitagawa, *J. Org. Chem.*, 1991, **56**, 5007; (*c*) K. T. Liu, S. J. Hou and M. L. Tsao, *J. Org. Chem.*, 1998, **63**, 1360; (*d*) K. T. Liu, S. J. Hou and M. L. Tsao, *J. Chin. Chem. Soc.*, 2009, **56**, 425; (*e*) K. I. Takeuchi, Y. Ohga, M. Yoshida, K. Ikai, T. Shibata, M. Kato and A. Tsugeno, *J. Org. Chem.*, 1997, **62**, 5696; (*f*) K. Takeuchi, Y. Ohga, T. Ushino and M. Takasuka, *J. Phys. Org. Chem.*, 1997, **10**, 717.

9 (*a*) D. A. Ponomarev and V. V. Takhistov, *J. Chem. Educ.*, 1997, **74**, 201; (*b*) R. Fuchs, *J. Chem. Educ.*, 1984, **61**, 133; (*c*) S. E. Wheeler, K. N. Houk, P. v R. Schleyer and W. D. Allen, *J. Am. Chem. Soc.*, 2009, **131**, 2547.

10 E. Blokker, W.-J. van Zeist, X. Sun, J. Poater, J. M. van der Schuur, T. A. Hamlin and F. M. Bickelhaupt, *Angew. Chem., Int. Ed.*, 2022, **61**, e202207477.

11 (*a*) P. Vermeeren, S. C. C. van der Lubbe, C. Fonseca Guerra, F. M. Bickelhaupt and T. A. Hamlin, *Nat. Protoc.*, 2020, **15**, 649; (*b*) P. Vermeeren, T. A. Hamlin and F. M. Bickelhaupt, *Chem. Commun.*, 2021, **57**, 5880.

12 (*a*) H. S. Andrei, N. Solcà and O. Dopfer, *Angew. Chem., Int. Ed.*, 2007, **47**, 395; (*b*) B. G. Oliveira, M. L. Vasconcellos and R. R. Olinda, *Struct. Chem.*, 2009, **20**, 81.

13 (*a*) T. A. Hamlin, B. van Beek, L. P. Wolters and F. M. Bickelhaupt, *Chem. – Eur. J.*, 2018, **24**, 5927; (*b*) T. Hansen, J. C. Rooze, F. M. Bickelhaupt and T. A. Hamlin, *J. Org. Chem.*, 2022, **87**, 1805.

14 (*a*) H. C. Brown, *J. Am. Chem. Soc.*, 1945, **67**, 374; (*b*) J. S. Lomas, M. J. D'Souza and D. N. Kevill, *J. Am. Chem. Soc.*, 1995, **117**, 5891; (*c*) K. Takeuchi, Y. Ohga and T. Kitagawa, *J. Org. Chem.*, 1991, **56**, 5007.

15 W.-J. van Zeist and F. M. Bickelhaupt, *Phys. Chem. Chem. Phys.*, 2009, **11**, 10317.